
Detecting Anomalous Faces with ‘No Peeking’ Autoencoders

Anand Bhattad¹ Jason Rock¹ David Forsyth¹

Abstract

Detecting anomalous faces has important applications. For example, a system might tell when a train driver is incapacitated by a medical event, and assist in adopting a safe recovery strategy. These applications are demanding, because they require accurate detection of rare anomalies that may be seen only at runtime. Such a setting causes supervised methods to perform poorly. We describe a method for detecting an anomalous face image that meets these requirements. We construct a feature vector that reliably has large entries for anomalous images, then use various simple unsupervised methods to score the image based on the feature. Obvious constructions (autoencoder codes; autoencoder residuals) are defeated by a ‘peeking’ behavior in autoencoders. Our feature construction removes rectangular patches from the image, predicts the likely content of the patch conditioned on the rest of the image using a specially trained autoencoder, then compares the result to the image. High scores suggest that the patch was difficult for an autoencoder to predict, and so is likely anomalous. We demonstrate that our method can identify real anomalous face images in pools of typical images, taken from celeb-A, that is much larger than usual in state-of-the-art experiments. A control experiment based on our method with another set of normal celebrity images - a ‘typical set’, but non-celeb-A are not identified as anomalous; confirms this is not due to special properties of celeb-A.

1. Introduction

We describe a method for detecting anomalous faces in images. Our method uses a novel representation of appearance (auto-encoder residuals), and does not require any example anomaly in training. We demonstrate that our method significantly improves over a number of natural baselines.

¹University of Illinois, Urbana-Champaign. Correspondence to: Anand Bhattad <bhattad2@illinois.edu>.

Detecting anomalous faces has important applications. For instance, a machine operator might fall asleep or have a heart attack. Ideally, a monitoring system would identify this kind of problem by watching the operator’s face and trigger some form of intervention. The crucial difficulty in building such a system is that there aren’t datasets showing (say) people having heart attacks. Moreover, a reliable anomaly detection system must be built without seeing actual anomalies to generalize well.

This example presents serious difficulties for current methods for anomaly detection (briefly reviewed below), because previous anomaly detection systems tend to be evaluated on datasets where anomalies are very different from typical examples. But anomalous faces look quite similar to typical faces. Our method requires a representation of face appearance which exaggerates the relatively small changes that make a face image anomalous, without actually being shown. Worse, because face images are relatively high dimensional, there is no practical prospect of simply applying a density estimator to the example images. Our strategy is to learn a compression procedure that reconstructs faces well, but not other similar unseen images, and then look at the residuals. This is not a routine application because one must be sure that (a) training images reconstruct well (routine) but (b) other similar images do not (tricky, and unusual). We show that a carefully designed residual of a specially trained autoencoder has these two properties and therefore provides a strong feature for identifying facial anomalies.

Contributions: We augment the Celeb-A dataset (Liu et al., 2015) for evaluating image anomaly detection. We present a novel feature learning approach for anomaly detection using inpainting auto-encoders. We build a dataset of real anomalous faces and real typical faces to evaluate the proposed framework. We demonstrate that our feature works well in both supervised and unsupervised applications.

2. Background

Anomaly detection has widespread applications, including: image matting (Hasler et al., 2003); identifying cancerous tissue (Alpert & Kisilev, 2014); finding problems in textiles (Serdaroglu et al., 2006; Mak et al., 2005); and preventing face spoofing (Arashloo et al., 2017). There is a recent survey in (Chandola et al., 2009). There are two distinct types

of approach in the literature. In one approach, examples of both inliers and outliers are available, and discriminative procedures can be used to build representations and identify and select features. In the other, one can model only inliers, and anomalies are available only at test time.

Face anomaly detection is a good example problem because (a) data resources of typical faces are abundant and (b) anomalous faces look a lot like typical faces; trivial methods perform poorly. We do not assume that anomalous faces are available at training time, because doing so creates two problems. First, anomalous face images are rare (which is why they’re anomalous) and highly variable in appearance, so a dataset of reasonable size is difficult to build. Second, the estimate of the decision boundary produced by any particular set of anomalous face images is likely to be inaccurate. The location of the decision boundary is determined by both the anomalies and the typical images; but the anomalies must be severely undersampled, and so contribute significant variance to the estimate of the decision boundary.

Instead, we assume that only typical faces are available at training time. We must now build some form of distribution model for true faces and exploit it to tell how uncommon the current image is. We focus on building a feature construction that allows simple mechanisms to compute an anomaly score. An alternative is to use a kernel method to build a distribution model (the **one-class SVM** of (Schölkopf et al., 2000)). We use this method as a baseline.

Our feature construction uses an **autoencoder** (Hinton & Salakhutdinov, 2006). Auto encoders use an encoder to compress a signal to a code, which can then be decompressed. The code is a low dimensional representation of content which has been shown to be useful for tasks such as: appearance editing (Yan et al., 2016; Lample et al., 2017); inpainting (Pathak et al., 2016); and colorization (Deshpande et al., 2017). Generative adversarial networks (GAN) (Goodfellow et al., 2014) have been used for anomaly detection in (Schlegl et al., 2017), but one must build a distribution for the code. (Schlegl et al., 2017) do explore using residuals in combination with the code likelihood. However, because their model is built on a GAN, their inference procedure is quite expensive, requiring many backprop and gradient steps, while our method is simply a forward run through an autoencoder. Our model also introduces a novel inpainting conditioning strategy for feature construction.

Evaluating anomaly detectors is tricky, because anomalies are rare. One strategy is to regard one class of image as typical, and another as anomalous. This strategy is popular (Zhai et al., 2016; Kliger & Fleishman, 2018; Deecke et al., 2018; Jindong Gu & Tresp, 2018) but may mislead. The danger is that one may unknowingly work with two very different classes, meaning that the quality of the distribution model for the typical class is not tested. In contrast, face

anomaly detection has the advantage of being (a) intrinsically useful and (b) clearly difficult.

The set building method of (Zaheer et al., 2017) could be applied to face anomaly detection. This approach has been shown to be accurate at identifying the one special face in a set of 16. A direct comparison is not possible, because their method relies on identifying the one different face in a set (i.e. given 15 smiling faces and one frowning face, it should mark the frowning face). However, we adopt their evaluation methodology and use analogous scoring methods.

3. Anomaly Features

We view anomaly detection as feature construction followed by a simple unsupervised method. Natural choices of feature constructions are autoencoder codes, pretrained discriminative models (eg (Cao et al., 2017)), or autoencoder residual features. An anomalous face image will look mostly like a typical face image, but will display some crucial differences. The problem is we don’t know where those differences are or what they look like. A natural strategy is based on a generative models of typical face images. Write Q for a test image, and $\mathcal{M}(Q; \theta)$ for a learned model that produces the typical face image that is ‘closest’ to the query image. We could then use the difference $\mathcal{M}(Q; \theta) - Q$ to compute a score of anomaly. In practice, “peeking” by the learned model (details below) means that this approach fails. The learning procedure results in a model that is biased to produce a $\mathcal{M}(Q; \theta)$ that is closer to Q than it should be.

A simple variant of this approach is extremely effective. Rather than requiring $\mathcal{M}(\cdot; \theta)$ to make the closest typical image, we conceal part of Q from $\mathcal{M}(\cdot; \theta)$ and require it to extrapolate. We then compare the extrapolated region to Q to produce the anomaly signal.

3.1. Autoencoder Residuals as Anomaly Signals

We will build \mathcal{M} using an autoencoder. Autoencoders construct low dimensional latent variable models from high dimensional signals. An encoder \mathcal{E} estimates the latent variable (code; z) for a given input Q ; a decoder \mathcal{D} recovers the signal from that code. The two are trained together, using criteria like the accuracy of the signal recovery (ie $|\mathcal{D}(\mathcal{E}(Q)) - Q|^2$; (Bengio et al., 2009)). Variational versions which use Bayes priors on the code have been explored as well (Kingma & Welling, 2014). As we show in table 1, the code produced by the encoder is a poor guide to anomaly, likely because it is still fairly high in dimension, and an appropriate distribution model is obscure (Schlegl et al., 2017). The autoencoder image reconstruction residual, $\mathcal{D}(\mathcal{E}(Q)) - Q$, is an alternative.

Straightforward experiments establish that the residual is

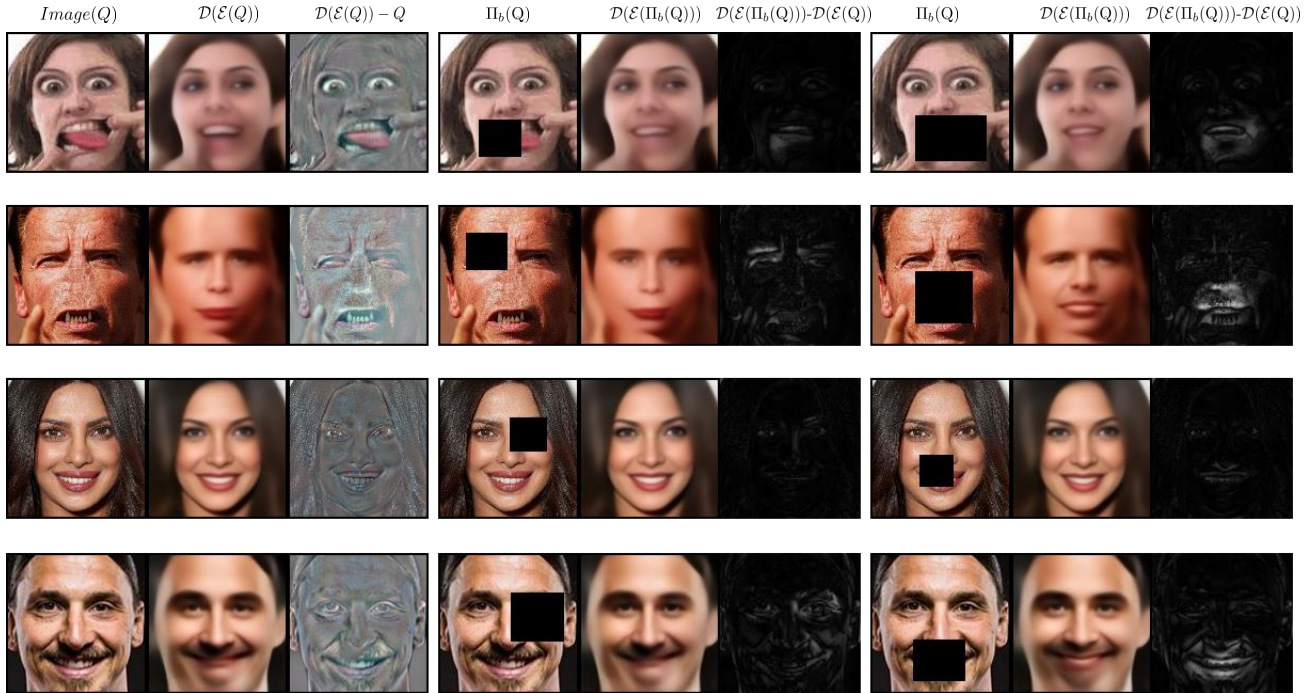


Figure 1. Forcing an autoencoder to inpaint at test time has important effects on the reconstruction. **Top two rows:** anomalous face images; **bottom two rows** typical face images. In the **first column**, the three images are actual input images, autoencoder’s reconstructed images and the autoencoder residuals respectively. In the **second and third column**, the first image is the masked input, second is the autoencoder’s reconstructed images and third is the residual difference between inpainted reconstruction residual from the residuals in the the first column. Notice how, for anomalous faces, not showing the autoencoder the content of the box affects the reconstruction. In the top row, attend to the dark bar at the left side of the model’s mouth, significantly reduced when the autoencoder reconstructs without seeing Q (i.e. no peeking). Similarly, concealing the whole mouth results in a much more conventional reconstruction of the mouth. As a result, the residual error emphasizes where the image is anomalous. For the second row, note how eye size and gaze are affected; and the significant change in reconstructed mouth shape when the mouth is concealed. This effect is minor for typical faces. As a result, residuals against autoencoder inpainting are strong cues to anomaly.

a poor anomaly signal (Figure 1). The reason is interesting. An autoencoder is trained to reproduce signals from its training set, but this regime does not necessarily discourage reproducing other images as well. An autoencoder that is trained to reproduce face images accurately has not been trained *not* to reproduce (say) cat images accurately, too. This means the autoencoder could reduce the training loss by adopting a compression strategy that works for many kinds of images. Therefore, a compression procedure that is good at compressing face images is not necessarily bad at compressing other images. This problem is not confined to neural networks. For example, choice of principal components that represents face images well (Sirovich & Kirby, 1987) may represent (say) cat images. Denoising in current implementations (Vincent et al., 2010) does not cure this problem. For example, a good denoising strategy is to construct a large dictionary of patches, then report the closest patch to the input. While a dictionary built on faces may reproduce some classes of image poorly, there is no guar-

antee in the training loss. Requiring a ‘small’ code (Hinton & Zemel, 1994) or adding code regularization (Kingma & Welling, 2014) does not cure this problem either, because it is not known how to account for the information content of the code. As a result, the model \mathcal{M} built by the autoencoder is not guaranteed to report the typical face image that is ‘closest’ to the query image; instead, it may pass through some of the query image as well (‘peeking’ at the query image), so resulting in a small residual and a poor anomaly signal. Experimental experience suggests that neural networks quite reliably adopt unexpected strategies for minimizing loss (‘cheating’ during training), meaning that we expect peeking to occur, and figure 1 confirms that it does. Peeking can be overcome by forcing the autoencoder to fill in large holes in the query image.

4. Beating Peeking with Inpainting

Write Π_b for an operator that takes an image and overwrites a box b with zeros; write $\Pi_{\bar{b}}$ for an operator that overwrites all but the box b with zeros. These boxes will be quite large in practice. We will train an autoencoder $(\mathcal{E}, \mathcal{D})$ as below. We build an anomaly feature vector by constructing $|\Pi_{\bar{b}}[\mathcal{D}(\mathcal{E}(\Pi_b(Q))) - Q]|$ for a variety of boxes (as below). We will then apply simple decision procedures to this feature.

This feature works because the autoencoder cannot peek into Q within the box. Instead, it must extrapolate into b , and that extrapolation is difficult to produce for multiple classes. In turn, the extrapolate is a much better estimate of what a typical face image would look like within b , conditioned on the rest of Q . For example, if b spans a mouth, then the autoencoder constructs a typical mouth conditioned on the face and compares it with the observed mouth, and if the mouth is anomalous the residual will be large (Figure 1).

This is similar to the inpainting problem explored in (Pathak et al., 2016), though we do not use an adversarial loss. The autoencoder is trained to inpaint randomly selected boxes. We use $|\mathcal{D}(\mathcal{E}(\Pi_b(Q))) - Q|_1$ as a training loss, thus requiring the autoencoder to inpaint. The only difference between this and a denoising regime is the size of the boxes, which is large compared to gaussian noise.

Our encoder and decoder use standard convolutional architectures with a fully connected layer for code construction. Average pooling is used for downsampling, and bilinear interpolation is used for upsampling. Following (Berthelot et al., 2017), we use a higher capacity network for the encoder than the decoder which seems to help with reconstructing higher frequency information. We use the elu non-linearity and batch normalization after each conv layer, and a tanh non-linearity on the output from the decoder. We use the L_1 norm for our training loss.

5. Eyeglass Experiment

Poor feature performance on a supervised task suggests that unsupervised methods will perform poorly too. Therefore in evaluating feature constructions, it can be useful to compare to an oracle. To do so, we construct a proxy anomaly experiment, where anomalous faces are those wearing eyeglasses, so allowing discriminative training of the oracle. Our oracle takes the form of a supervised L_1 -regularized linear regressor (we use glmnet (Friedman et al., 2010)) trained on data. While poor performance on the oracle suggests that unsupervised methods will perform poorly too, good performance on the oracle is not necessarily indicative of good unsupervised performance. We therefore also explore natural choices for unsupervised methods including one-class SVM (Schölkopf et al., 2000), one-class density estimates

L_1 Regularized Logistic Regressor			
Feature	Resnet50	AE Code	Res Patch
Accu	99.4	85.6	93.5

1-Class SVM			
Feature	Resnet50	AE Code	Res Patches
AUC	52.3	51.8	53.8

Mahalanobis Distance			
Feature	Resnet50	AE Code	Res Patches
AUC	52.8	50.8	92.5

L_∞ norm			
Feature	Resnet50	AE Code	Res Patches
AUC	NA	NA	81.5

Table 1. Supervised and unsupervised glasses detection with our features. We compare our inpainting residual features, **Res patch** to codes from the autoencoder and state of the art Resnet features trained on face detection. We note that Resnet features work extremely well for supervised tasks, in fact in our simple dataset, Resnet features combined with an L_1 regularized logistic regression performs nearly perfectly. However Resnet features do not perform well for either of the unsupervised classifiers. On the other hand, the inpainting residual features perform better than the autoencoder code regardless of the classifier type, and perform far better than Resnet for unsupervised classifiers.

such as Mahalanobis Distance (Mahalanobis, 1936), and heuristic methods such as the L_∞ norm which are meaningful for our residual based feature.

We use the Celeb-A dataset (Liu et al., 2015), which is a collection of thousands of labeled faces. As in (Berthelot et al., 2017), we filter and crop with the Viola-Jones face detector (Viola & Jones, 2001), resulting in frontal faces in tightly cropped 128x128 boxes. For this experiment, we use 7700 images of people wearing eyeglasses as anomalies and 7000 images without eyeglasses as our unsupervised training set. We train our inpainting autoencoder with random Π_b for each sample on 90% of the non-eyeglass data. During test we use the same model to construct autoencoder codes as well as the inpainting features. For inpainting features, we use 32x32 boxes in a regular grid. We exclude the boxes that would lie directly on the image boundary. For Resnet features we use a pretrained resnet trained on face recognition from (Cao et al., 2017), we remove the final softmax layer, and use the resulting network as a feature constructor.

Our results shown in table 1 suggest that inpainting autoencoder residuals contain sufficient information for attribute classification. One class SVM’s are not a strong baseline for this problem. Mahoanobis distance is a decent baseline for our features. Inpainting autoencoder residual images are informative, even with the simplest heuristic classifier L_∞ .

We also show that autoencoder codes are less adept than inpainting residuals.

It is not surprising that the L_∞ classifier works so well. Each inpainting feature is a local anomaly detector for the content under the box. Since the inpainting autoencoder was trained on images without glasses, when the box covers the eyeglasses, the inpainted content will not have eyeglasses. Consequently, the residual will be large. Taking the L_∞ norm reports the score from the most violated box. Note that this experiment is not a true anomaly experiment, but it is similar to previous work (Zhai et al., 2016; Kliger & Fleishman, 2018; Deecke et al., 2018; Jindong Gu & Tresp, 2018) which uses attributes or class labels as proxies for anomalies.

6. Anomaly Experiment

We wish to determine whether we can detect true anomalies in a realistic setting. We use the Celeb-A dataset as our training data, filtering and cropping for frontal faces using Viola-Jones as in section 5. However rather than considering any specific attribute, we consider the entire Celeb-A dataset as typical data. We set aside 30,000 images for use in test, leaving us with 125,253 images for training. For our anomaly images, we collect a 100 image anomaly dataset. This set, which we call the **anomaly set** is comprised of strange or “weird” faces (Figure 2c). It includes extreme makeup, masks, photoshops, and people making extreme faces. We pass the images through the same Viola-Jones detector and cropper. This rejects many of the anomaly images, and in fact we only have about a 3% yield on anomaly images, meaning that we had to find roughly 3000 anomaly images in order to get 100. However, this construction is sensible: if Viola-Jones does not believe the images have a face, then they are too obviously anomalous. For example, a photograph of a cat would have a high anomaly score under our method, but a cat is also not likely to be identified as a face by a competent detector, so determining it is an anomaly is not particularly important or difficult.

We also wish to determine if anomaly detection is caused by special features of the Celeb-A dataset. An anomaly detector which identifies any image not from Celeb-A would not be particularly useful. We therefore collect a **typical set** of 100 images we do not believe to be anomalous images. It is comprised of pictures of celebrities that were taken after Celeb-A was created so there are no overlaps in pictures (Figure 2b). We also tried to find new celebrities, so that the people would be less likely to have appeared in the original Celeb-A dataset. This dataset is used to validate that a method is not memorizing images in Celeb-A or finding a particular feature of Celeb-A and rejecting any new images. We show samples from Celeb-A, the typical set and the anomaly set in figure 2. By example it is reasonable to ask

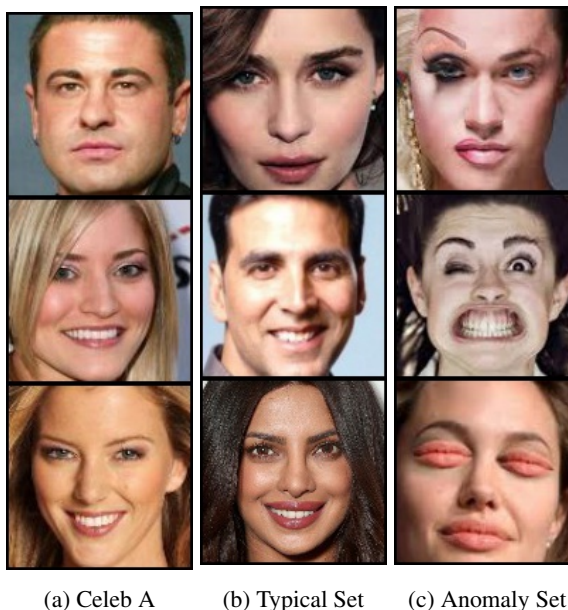


Figure 2. Images from celeb A 2a, from the **typical set** 2b and from the **anomaly set** 2c. It is very clear when an image is an anomaly and when it is not. Our typical set is similar to celeb-A with recent new images collected after celeb-A was created, ensuring no overlaps with celeb-A images. However, there are some slight features of Celeb-A images that are noticeably different from our typical set. For example, the resolution of the images seems to be slightly different.

an anomaly detection method to identify images from the anomaly set without identifying images from the typical set.

Our experiments are modeled on the set experiment presented in (Zaheer et al., 2017). They form a set of 16 images from Celeb-A where 15 images share at two attributes, and one image differs. The goal is to identify the image with different attributes. We adjust this slightly. Large sets are more indicative of performance for real world anomaly detection, where the goal is to identify one image in thousands rather than one image in ten. However, using large sets is significantly more difficult so we report recall at 1, 5, and 10 rather than just reporting recall at 1. Note that at no point does any method have access to labels, which are revealed only to evaluate the experiment. We believe this is a better model for detecting rare anomalies.

Evaluating anomaly detection: We select one image from the anomaly set, and between 15 and 299 images from the 30,000 celeb-A held out images (without consideration of attributes, in contrast to (Zaheer et al., 2017)). We then score each image using our feature and a variety of scoring methods (section 6.1) to evaluate recall for the anomaly image, averaged over 10,000 sets. As figure 4 shows, recall is strong even from large sets, and the choice of score appears not to matter.

Control: Strong results could be caused by some special feature of celeb-A images. To control for this possibility, we repeat the anomaly detection experiment, but replacing the image from the anomaly set with an image from the typical set (100 typical images not from celeb-A). If celeb-A were wholly representative, then this experiment should produce recalls at chance. As figure 4 shows, the results are not at chance (there is something interesting lurking in celeb-A), but recall is very much weaker than for anomalies. The performance of the anomaly detector cannot be explained by quirks of celeb-A

6.1. Unsupervised Feature Learning

We use our regular grid of residual features for 32x32 patches with a 32 pixel edge exclusion and explore a variety of methods for turning the residual features into an anomaly score. The L_∞ norm over the feature vector makes up our main method due to its simplicity and good performance. It is not obvious that this is a good choice, and for a general feature, this norm would be largely meaningless. However, as demonstrated in the attribute classification task our features are designed to be well suited to this norm. For our feature, the L_∞ norm finds the most violated residual from the set of patches, which is obviously useful for anomalies that tend to occur locally.

The **Mahalanobis Distance** (mahal) estimates a mean and covariance from a set and then measures distance with respect to the mean and covariance. It is typical to estimate the mean and covariance on training data. The **Equivariant Transform** (equivariant) introduced in (Zaheer et al., 2017) can be applied in an unsupervised manner on a set of images. A sensible version looks like the Mahalanobis Distance. Recall the equivariant transform in matrix form:

$$\mathbf{X} = [\lambda\mathbf{I} + \gamma(\mathbf{1}\mathbf{1}^T)] \mathbf{X} \quad (1)$$

Which for an element x_i is equivalent to

$$\hat{x}_i = \lambda x_i + \gamma \sum_i x_i \quad (2)$$

Let Σ^{-1} be the inverse covariance of \mathbf{X} , then $\gamma = -\Sigma^{-1/2}/N$ and $\lambda = \Sigma^{-1/2}$ compute a transformation which under the L_2 is the Mahalanobis Distance. This transformation is sensible and can be applied to the data prior to applying the L_∞ norm to reweight the feature dimensions and take into account that some dimensions might be highly varying while others are not. For our autoencoder residual feature, we assume that our features are IID, so we can estimate a diagonal covariance, and we compute a robust mean and covariance by eliminating the largest and smallest values on each feature. Note that this is done without knowing which item is anomalous and thus does not violate train-test splits.

The **Local False Discovery Rate** (lfd_r) is a construction that identifies the probability that an item comes from a null distribution, without knowing what the null is (Efron, 2007). The method originates in multiple hypothesis testing, assuming that most observations come from the null. Assume the null distribution is $f_o(z)$, the non-null is $f_1(z)$, and the prior an item comes from the null is π_o . Then the lfd_r is

$$p(\text{null}|z) = \frac{\pi_o f_o(z)}{\pi_o f_o(z) + (1 - \pi_o) f_1(z)} \quad (3)$$

Small values suggest an item is worth investigating (i.e., anomalous). Estimation is complicated by the fact that neither $f_o(z)$ nor $f_1(z)$ are known; but the assumption that π_o is large, and $f_o(z)$ is ‘close’ to a standard normal distribution allows fairly accurate estimation. We used the R program `locfdr`. We estimated local false discovery rates using all 30200 test data items (doing so does not involve knowing which item is anomalous, so does not violate test-train protocols). We estimate using a standardized version of the L-infinity score, and a standardized version of the log of the L-infinity score.

6.2. Results

As seen in figure 4, our feature performs well regardless of feature transformation applied. We report performance from (Zaheer et al., 2017) on the graph, even though their experiment is on different data. While they outperform our method for 16 image sets, using our auto-encoder residual features, we identify **anomalies** at rates significantly greater than chance even as the size of the set increases. Resnet-50 features (Cao et al., 2017) with a Mahalanobis Distance represents a strong baseline, however, we outperform it. There does seem to be some bias in the Celeb-A dataset being used to identify anomalies but our features and the Resnet-50 features do not identify **typical** images at anywhere near the same rate as anomalies. The gap between performance on typical images and anomalous images is apparent and clearly significant (eg. 40 vs 20 percent for recall at 1 in a 16 image set).

For qualitative comparison, we show the median image from each decile ranked by their L_∞ anomalous score in figure 3. We also show a plot of how frequently they are ranked in the top images in a set of increasing size. Anomaly images are frequently identified as the most anomalous image in a 16 image set and as a top 10 anomalous image in 128 image sets. Typical images are almost never identified as the most anomalous image in any set, and almost never identified as the top 10 in any set larger than 16. The median least anomalous image is roughly as anomalous as the median typical image. These findings are consistent with our quantitative results, which show that images from the anomalous set are identified frequently and images from the typical set are identified more often than chance, but frequently less

Detecting Anomalous Faces with ‘No Peeking’ Autoencoders

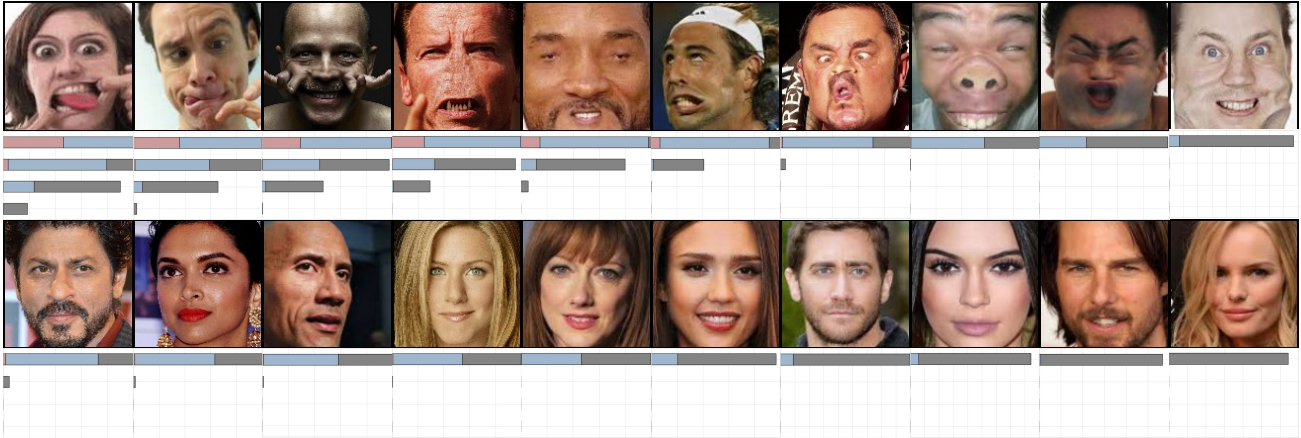


Figure 3. **Top row:** images from the anomaly set sorted by their L_∞ anomaly scores. The median image from each decile. **Bottom row:** images from the ordinary set sorted by their L_∞ anomaly scores. The median image from each decile is shown. Bar charts below show how frequently the image was identified @1 (red), @5 (blue), and @10 (gray) for (top to bottom) 16, 64, 128, and 256 image sets. For anomaly images (top row), being identified frequently is better, for ordinary images (bottom row) being identified less is better.

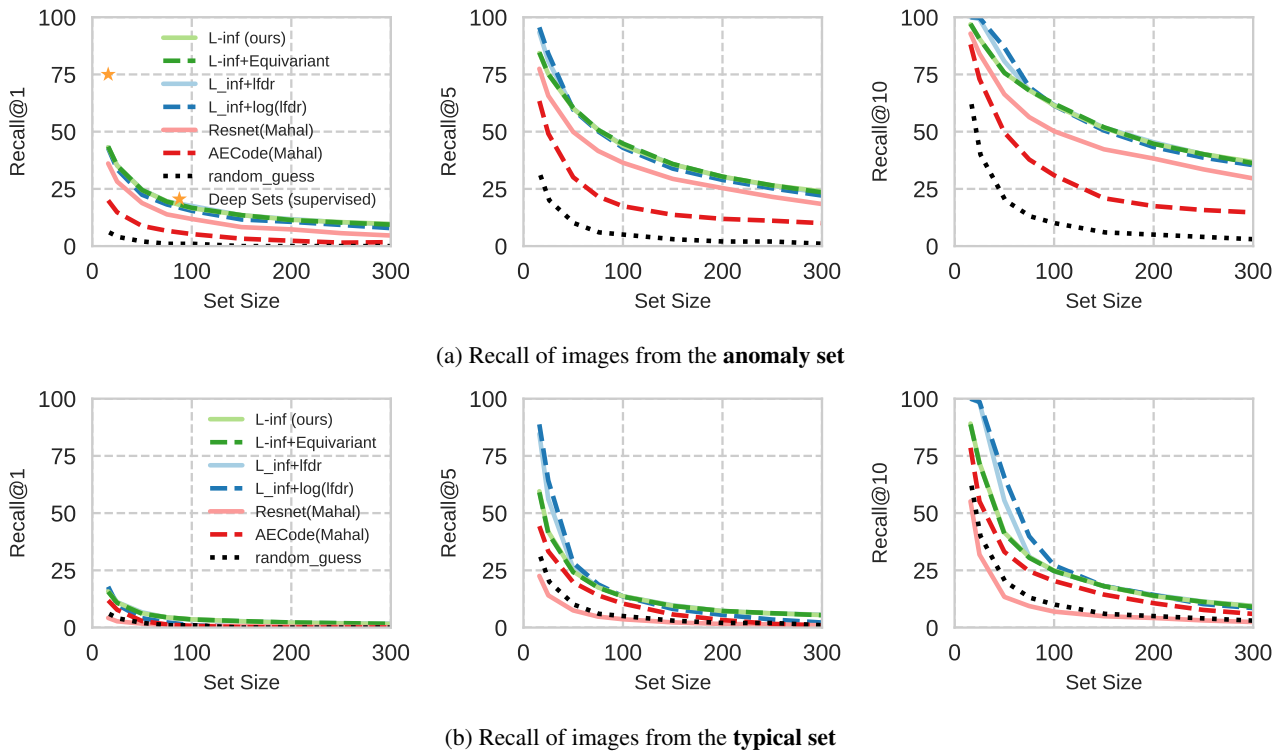


Figure 4. **Top row:** Recall at 1, 5, and 10 for various scores using our anomaly feature plotted against the size of the set from which the anomaly must be picked. We show the performance on our new data set for L_∞ on the autoencoders’ inpainted features, adding equivariant transformation to our features, local false discovery rate (lfdr and $\log(\text{lfdr})$), and Mahalanobis distance on features drawn from Resnet50 and autoencoder’s code as our baseline. Recalls are averaged over 10000 trials, and so have very low variance. Note there is very little visible difference between the performance of the scores, all of which beat chance very strongly. The equivariant transformations does not have any major effect to the performance and our feature construction method in itself encodes a strong representation of anomaly. The star in the Recall@1 figure is reproduced from the work of Deep Sets (Zaheer et al., 2017). Though, there is no direct comparison of our method to Deep Sets, the difference in performance is an indicator of the gap between supervised and unsupervised methods. Note also the test is demanding compared to the literature; a single anomalous face must be picked from up to 300 others. However, these results might depend on some signal property of the celeb-A dataset. **Bottom row** shows results from our control experiment, where the image used as an anomalous image is a typical face image that doesn’t appear in celeb-A (details in section 6). Performance is not at chance (suggesting that celeb-A images have some hitherto not noted special properties) but is close. In particular, the performance of the anomaly detector on anomalous images very strongly exceeds its performance on control images, and so cannot be explained by the special properties of celeb-A (whatever they are).

often than true anomalies.

7. Conclusion

We introduce the inpainting autoencoder residual as a feature for combating the overgeneralization of compression losses. This allows us to train our method solely on non-anomalous data, mimicking how a real anomaly detector must be trained. We demonstrate that our inpainting residual features are useful and work well in supervised and unsupervised settings. Though we did not see improvement in performance, it is easy to use inpainting autoencoder features with various feature transformation techniques. We also describe a standard anomaly detection experiment for evaluating future anomaly work on image sets, enabled through the collect two small datasets to augment Celeb-A.

References

- Alpert, Sharon and Kisilev, Pavel. Unsupervised detection of abnormalities in medical images using salient features. In Ourselin, Sebastien and Styner, Martin A (eds.), *SPIE Medical Imaging*, pp. 903416–7. SPIE, March 2014.
- Arashloo, Shervin Rahimzadeh, Kittler, Josef, and Christmas, William. An Anomaly Detection Approach to Face Spoofing Detection: A New Formulation and Evaluation Protocol. *IEEE Access*, 5:13868–13882, 2017.
- Bengio, Yoshua et al. Learning deep architectures for ai. *Foundations and trends® in Machine Learning*, 2(1): 1–127, 2009.
- Berthelot, David, Schumm, Tom, and Metz, Luke. Began: Boundary equilibrium generative adversarial networks. *arXiv preprint arXiv:1703.10717*, 2017.
- Cao, Qiong, Shen, Li, Xie, Weidi, Parkhi, Omkar M, and Zisserman, Andrew. Vggface2: A dataset for recognising faces across pose and age. *arXiv preprint arXiv:1710.08092*, 2017.
- Chandola, Varun, Banerjee, Arindam, and Kumar, Vipin. Anomaly Detection: A Survey. *Acm Computing Surveys*, 41(3), 2009.
- Deecke, Lucas, Vandermeulen, Robert, Ruff, Lukas, Mandt, Stephan, and Kloft, Marius. Anomaly detection with generative adversarial networks, 2018. URL <https://openreview.net/forum?id=S1EfylZ0Z>.
- Deshpande, Aditya, Lu, Jiajun, Yeh, Mao-Chuang, Chong, Min Jin, and Forsyth, David. Learning Diverse Image Colorization. In *2017 IEEE Conference on Computer Vision and Pattern Recognition (CVPR)*, pp. 2877–2885. IEEE, 2017.
- Efron, Bradley. Size, power and false discovery rates. *Ann. Statist.*, 35(4):1351–1377, 08 2007. doi: 10.1214/009053606000001460. URL <https://doi.org/10.1214/009053606000001460>.
- Friedman, Jerome, Hastie, Trevor, and Tibshirani, Robert. Regularization paths for generalized linear models via coordinate descent. *Journal of Statistical Software*, 33(1): 1–22, 2010. URL <http://www.jstatsoft.org/v33/i01/>.
- Goodfellow, Ian J, Pouget-Abadie, Jean, Mehdi, Mirza, Xu, Bing, Warde-Farley, David, Ozair, Sherjil, Courville, Aaron, and Bengio, Yoshua. Generative Adversarial Networks. In *NIPS*, June 2014.
- Hasler, D, Sbaiz, L, Susstrunk, S, and Vetterli, M. Outlier modeling in image matching. *IEEE TPAMI*, 25(3):301–315, March 2003.
- Hinton, Geoffrey E and Salakhutdinov, Ruslan R. Reducing the dimensionality of data with neural networks. *science*, 313(5786):504–507, 2006.
- Hinton, Geoffrey E and Zemel, Richard S. Autoencoders, minimum description length and helmholtz free energy. In *Advances in neural information processing systems*, pp. 3–10, 1994.
- Jindong Gu, Matthias Schubert and Tresp, Volker. Semi-supervised outlier detection using generative and adversary framework, 2018. URL <https://openreview.net/forum?id=BkS3fnl0W>.
- Kingma, Diederik P and Welling, Max. Auto-Encoding Variational Bayes. In *ICLR*, 2014.
- Kliger, Mark and Fleishman, Shachar. Novelty detection with GAN, 2018. URL <https://openreview.net/forum?id=Hy7EPh10W>.
- Lample, Guillaume, Zeghidour, Neil, Usunier, Nicolas, Bordes, Antoine, Denoyer, Ludovic, and Ronzato, Marc-Aurilio. Fader Networks: Manipulating Images by Sliding Attributes. *arXiv.org*, pp. 1–10, June 2017.
- Liu, Ziwei, Luo, Ping, Wang, Xiaogang, and Tang, Xiaoou. Deep learning face attributes in the wild. In *Proceedings of International Conference on Computer Vision (ICCV)*, December 2015.
- Mahalanobis, Prasanta Chandra. On the generalized distance in statistics. National Institute of Science of India, 1936.
- Mak, K L, Peng, P, and Lau, H Y K. A real-time computer vision system for detecting defects in textile fabrics. In *2005 IEEE International Conference on Industrial Technology*, pp. 469–474. IEEE, 2005.

- Pathak, Deepak, Krähenbühl, Philipp, Donahue, Jeff, Darrell, Trevor, and Efros, Alexei A. Context Encoders: Feature Learning by Inpainting. In *Computer Vision and Pattern Recognition*, April 2016.
- Schlegl, Thomas, Seeböck, Philipp, Waldstein, Sebastian M, Schmidt-Erfurth, Ursula, and Langs, Georg. Unsupervised anomaly detection with generative adversarial networks to guide marker discovery. In *International Conference on Information Processing in Medical Imaging*, pp. 146–157. Springer, 2017.
- Schölkopf, Bernhard, Williamson, Robert C, Smola, Alex J, Shawe-Taylor, John, and Platt, John C. Support vector method for novelty detection. In *Advances in neural information processing systems*, pp. 582–588, 2000.
- Serdaroglu, A, Ertuzun, A, and Ercil, A. Defect detection in textile fabric images using wavelet transforms and independent component analysis. *Pattern Recognition and Image Analysis*, 16(1):61–64, 2006.
- Sirovich, Lawrence and Kirby, Michael. Low-dimensional procedure for the characterization of human faces. *Josa a*, 4(3):519–524, 1987.
- Vincent, Pascal, Larochelle, Hugo, Lajoie, Isabelle, Bengio, Yoshua, and Manzagol, Pierre-Antoine. Stacked Denoising Autoencoders: Learning Useful Representations in a Deep Network with a Local Denoising Criterion. *The Journal of Machine Learning Research*, 11:3371–3408, December 2010.
- Viola, Paul and Jones, Michael. Rapid object detection using a boosted cascade of simple features. In *Computer Vision and Pattern Recognition*, volume 1. IEEE, 2001.
- Yan, Xinchen, Yang, Jimei, Sohn, Kihyuk, and Lee, Honglak. Attribute2Image: Conditional Image Generation from Visual Attributes. In *European Conference on Computer Vision*, 2016.
- Zaheer, Manzil, Kottur, Satwik, Ravanbakhsh, Siamak, Poczozos, Barnabas, Salakhutdinov, Ruslan R, and Smola, Alexander J. Deep Sets. In *NIPS*, pp. 3394–3404, 2017.
- Zhai, Shuangfei, Cheng, Yu, Lu, Weining, and Zhang, Zhongfei. Deep structured energy based models for anomaly detection. In *International Conference on Machine Learning*, pp. 1100–1109, 2016.